Contents lists available at ScienceDirect

Chemical Engineering Research and Design

journal homepage: www.elsevier.com/locate/cherd

Mathematical modeling of two-chamber batch microbial fuel cell with pure culture of *Shewanella*

Morteza Esfandyari, Mohmmad Ali Fanaei, Reza Gheshlaghi, Mahmood Akhavan Mahdavi*

Department of Chemical Engineering, Faculty of Engineering, Ferdowsi University of Mashhad, Mashhad, Iran

ARTICLE INFO

Article history:
Received 29 May 2016
Received in revised form 7 September 2016
Accepted 11 September 2016
Available online 13 October 2016

Keywords:
Microbial fuel cell
Mathematical modeling
Lactate
Shewanella
Batch

ABSTRACT

Microbial fuel cell (MFC) is a bioreactor which converts the chemical energy of organic compounds of chemical bonds to the electrical energy by catalytic reactions. In the current study a dynamic model is proposed, based on the direct transfer of electron for a two-chamber batch MFC at constant temperature, in which, lactate is used as the substrate, *Shewanella* as the microbial culture, and air as the input to the cathode chamber. The proposed model has many parameters. Some of these parameters are selected from the literatures and the others are estimated based on the experimental data. The required experimental data are prepared from a two-chamber MFC with working volume of $135 \times 10^{-6}\,m^3$ for each chamber at two substrate concentrations of 5.0 and $7.5\,kg\,m^{-3}$. Three kinetic models known as Monod, Backman, and Tessier are used for describing the microbial specific growth rate. The results show that the better prediction of substrate concentration can be observed by using a Monod model ($R^2 > 0.97$). The predicted voltage and current of the MFC by the proposed model have good agreement with experimental data.

1. Introduction

The predicted voltage and current of the batch microbial fuel cell and compared with experimental data. MFC is one of the novel methods for the energy production, in which microorganisms generate electricity by conducting the oxidation–reduction reactions of a substrate. In such cells the electrochemical energy is directly converted to electrical energy (Allen and Bennetto, 1993). Although the application of MFCs was initially introduced in 1911 (Potter, 1911), little developments were made till recent decades (Oh et al., 2004; Xuan et al., 2009). Since in MFCs microorganisms act as electron donors, contrary to common fuel cells, they operate in moderate temperature and pressure conditions. One of the advantages of MFCs is their ability in conversion of the chemical energy from a biological environment to electrical current. Biocatalysts are applied for the conversion of chemical to electrical energy in the design of MFCs (Chaudhuri and Lovley, 2003; Rabaey and Verstraete, 2005). In some types of MFCs bacteria can be used as catalyst or microorganism (Chaudhuri and Lovley, 2003; Min et al., 2005).

Common MFCs usually have an anaerobic anode chamber and an aerobic cathode one, which are separated by a proton exchange membrane, the electrons and protons are produced in anode chamber during the oxidation of substrate by the microorganism (Du et al., 2011; Picioreanu et al., 2008, 2010b). Protons pass through the membrane to the cathode chamber, while electrons move from anode to cathode via an external circuit, therefore bioelectricity is generated in the circuit (Fig. 1). A final electron acceptor is required to complete this cycle in the cathode chamber. Commonly, oxygen has been used as the electron acceptor in the cathode chamber due to the high oxidation–reduction potential and low operating cost (Chou et al., 2013; Fitzgerald et al., 2013).

Many researchers investigated the effect of a variety of carbon sources on MFC performance, but few studies were thoroughly focused on the kinetic analysis of the type and concentrations of substrate (Jafary et al., 2013; Reimers et al., 2007; Sedaqatvand et al., 2011; Stein et al., 2011).

Abbreviations: DO, dissolved oxygen; OTR, oxygen transfer rate; OUR, oxygen uptake rate; MFC, microbial fuel cell; UV, ultraviolet; OD, optical density.

* *Corresponding author.*
E-mail address: Fanaei@um.ac.ir (M.A. Fanaei).

http://dx.doi.org/10.1016/j.cherd.2016.09.016

Nomenclature

Symbol	
A_m	Area of membrane (m^2)
b	Tafel coefficient (mV)
b_{ina}	Inactivation coefficient (day^{-1})
b_{det}	Detachment coefficient (day^{-1})
$C_{CO_2 0}$	The initial concentration of carbon dioxide in bulk liquid ($kg\,m^{-3}$)
C_{H0}	The initial concentration of hydrogen in bulk liquid ($kg\,m^{-3}$)
$C_{CO_2 b}$	The concentration of carbon dioxide in bulk liquid ($kg\,m^{-3}$)
C_{Hb}	The concentration of hydrogen in bulk liquid ($kg\,m^{-3}$)
C_{O_2}	The concentration of oxygen in cathode chamber ($kg\,m^{-3}$)
C_{CO_2}	The concentration of carbon dioxide in biofilm ($kg\,m^{-3}$)
C^*	The equilibrium or saturation concentration of the oxygen ($kg\,m^{-3}$)
C_H	The concentration of hydrogen in biofilm ($kg\,m^{-3}$)
C_{HC}	The concentration of hydrogen in cathode chamber ($kg\,m^{-3}$)
C_{S0}	The initial concentration of lactate ($kg\,m^{-3}$)
C_{Sb}	The concentration of lactate in bulk liquid ($kg\,m^{-3}$)
C_S	The concentration of lactate in biofilm ($kg\,m^{-3}$)
D_{CO_2}	The diffusivity of carbon dioxide ($m^2\,day^{-1}$)
D_H	The diffusivity of hydrogen ($m^2\,day^{-1}$)
D_s	The diffusivity of lactate ($m^2\,day^{-1}$)
d_m	Membrane thickness (m)
d_{cell}	Distance between electrodes (m)
$E_{0,anode}$	Standard anode voltage (mV)
$E_{0,cathode}$	Standard cathode voltage (mV)
F	Faraday's constant ($Cmol^{-1}$)
i	Current (mA)
i_l	Limited current (mA)
$i_{0,ref}$	Exchange current in reference conditions (mA)
k_m	Membrane conductivity ($mS\,m^{-1}$)
k_{aq}	Solution conductivity ($mS\,m^{-1}$)
K_s	Half-max-rate lactate concentration ($kg\,m^{-3}$)
$k_L a$	The overall volumetric oxygen mass transfer coefficient (day^{-1})
L_f	The thickness of biofilm (m)
L_l	The thickness of the laminar diffusion sublayer
q_{O_2}	The specific uptake rate of oxygen (day^{-1})
r_{max}	Reaction rate constant (day^{-1})
T	Temperature (K)
V_l	Bulk liquid anode chamber volume (m^3)
Y_{ac}	The bacterial yield ($kg\,dry\,cell\,kg^{-1}$)
ϕ_a	Volume fraction of the active biomass
ϕ_i	Volume fraction of the inactive biomass
ρ	The biomass density ($kg\,m^{-3}$)
η_{ohm}	Ohmic overpotential (mV)
η_{act}	Activation overpotential (mV)
η_{conc}	Concentration overpotential (mV)

Stein et al. (2011) introduced a kinetic model for detection of toxicity in a MFC for application as biosensor.

Jafary et al. (2013) studied the inhibition effect in kinetic models of substrate consumption to evaluate the inhibition effect. Three kinetic models, namely, Tessier, Haldane and Aiba, accounted for the substrate inhibition, were chosen to fit the experimental data (Jafary et al., 2013). The predicted current and power densities of the MFC by the proposed model have good agreement with experimental data.

Reimers et al. (2007) introduced a kinetic model for intermediate substance in an MFC. The proposed model is in good agreement with experimental data.

Although a great number of experimental studies have been performed to achieve better understanding of the MFCs' performance, few researchers have focused on the modeling and simulation of the MFCs. One of the first modeling researches in this filed was conducted by Zhang and Halme in 1995 (Zhang and Halme, 1995). It was a one dimensional and dynamical model, with an external mediator (HNQ) for the electron transport.

Marcus et al. (2007) applied a one dimensional dynamic model considering the bioelectrochemical reaction of the MFC based on mass transfer, Ohm law, and Nerust–Monod kinetic model. Contrary to the other works, the direct conduction of electrons in biofilm under the electrical potential field was used.

The next model was presented for MFCs in 2007 by Picioreanu et al. (2007). The suspended microbial culture adhered on anode surface in one, two, and three dimensional coordinates was investigated in this model. In 2010, two studies were performed by Picioreanu et al. (2010a,b), in which the electron transport by the mediator was considered in their model. In this models, MFC behavior with suspended cells and the electron transport was studied. It was modeled based on mass transfer for some water soluble chemical species as a mediator oxidation and reduced substrate.

Wen et al. (2009) developed an electrochemical model for MFC based on the polarity curvature, which can be used for calculating the voltage drop change in various operational conditions.

Another model was presented by Zeng et al. (2010) for a two-chamber MFC with the acetate substrate in 2010. This model was introduced both for steady and dynamic states.

Pinto et al. in 2010 presented a model for anodophilic and methanogenic species (Pinto et al., 2010, 2012). Pinto's model was the simplified form of Picioreanu's model.

Kazemi et al. (2015) presented a dynamic one dimensional model of reverse MFC for production of acetate, CO_2, and water. This model was based on the Marcos et al.'s model (Marcus et al., 2007) in which the electrochemical reactions occurred in the cathode instead of anode, and biofilm was formed in the cathode.

In the most of investigations, the effects of different parameters on the performance of MFC were assessed. In all of them, except the Marcus et al.'s model (Marcus et al., 2007), the mechanism of electron transfer was based on the use of mediator materials. Whereas it is found that the electron transfer from microbe surface to electrode surface was done by the other methods. So, it is needed to consider the electron transfer method based on direct conduction. According to this issue, in the current work, direct electron transfer is assumed. In addition in most of the developed models the anode chamber of MFCs was considered in the modeling, while the significance of cathode chamber has been neglected. So, in this work, the whole MFC chambers are considered in the modeling, but for simplicity, lumped formulation is used.

In the following sections, after describing the materials and methods, kinetic model for the anode chamber was introduced. Further, mass balance in the liquid bulk and biofilm of the anode chamber

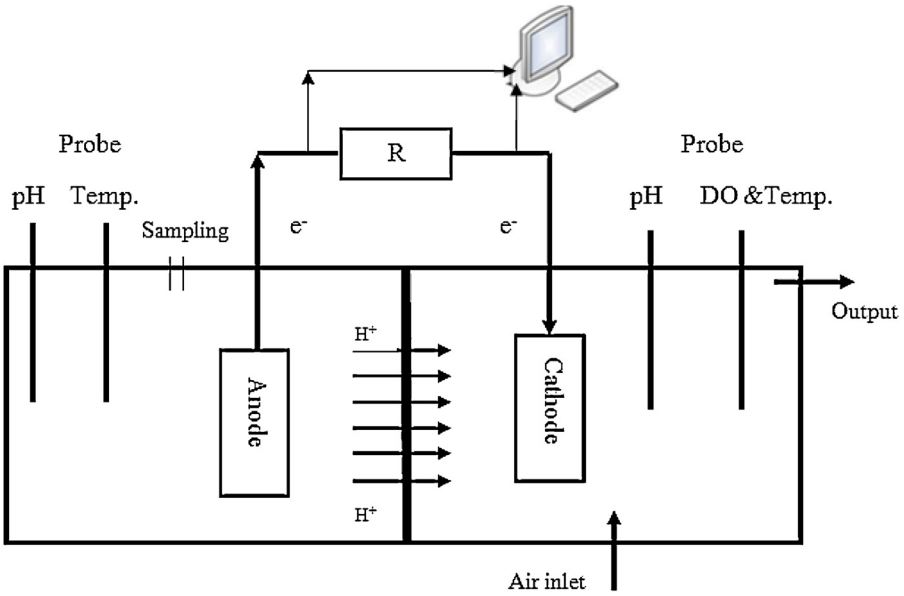

Fig. 1 – Structure of microbial fuel cell (Esfandyari et al., 2016).

were applied for substrate, CO_2 and H^+. In addition the mass balance is applied for oxygen consumption in the cathode chamber. According to these equations and electrochemical model, the voltage and current of MFC were determined. Finally, the experimental data and predicted results of the proposed model were presented.

2. Materials and methods

Two-chamber MFCs were made from an acrylic cylinder. The volume of each chamber was $15 \times 10^{-5}\,m^3$, with a working volume of $135 \times 10^{-6}\,m^3$. At the top of anode and cathode chamber, some ports were made for measuring pH, temperature, and other operational parameters (such as CO_2 concentration, dissolved oxygen concentration and substrate concentration). The electrodes were made of carbon felts (Panex35, Zoltek, USA). The anodic and cathodic sections were separated via a $32 \times 10^{-4}\,m^2$ cation exchange membrane (Ultrex CMI7000, Membranes Inter-national Inc., USA).

Batch experiments were carried out at pH of 7, initial substrate concentration of 5 or $7.5\,kg\,m^{-3}$, and a fixed external resistance of 100 Ω. The temperature of MFC was controlled at about 30 °C with tolerances of ±1.0 °C.

Bacteria *Shewanella* was supplied from *Iranian Research Organization for Science and Technology* (*IROST*). All experiments were conducted under strictly sterile conditions.

Anolyte medium was consist of $3\,kg\,m^{-3}$ NaOH, $1.5\,kg\,m^{-3}$ NH_4Cl, $0.1\,kg\,m^{-3}$ KCl, $0.6\,kg\,m^{-3}$ KH_2PO_4, $5.8\,kg\,m^{-3}$ NaCl, $0.01\,m^3\,m^{-3}$ mineral solution and $0.01\,m^3\,m^{-3}$ amino acid solution (adjust to pH of 7). Lactic acid was used as substrate (adjust to pH of 7). Before adding medium and substrate to each MFC, solutions were sterilized at 121 °C for 15 min in an autoclave (Watson and Logan, 2010).

The cathodic chamber of the MFC was filled with phosphate buffer solution of 25 mM ($2.678\,kg\,m^{-3}$ K_2HPO_4 and $1.310\,kg\,m^{-3}$ KH_2PO_4, adjusted to pH of 7) (Watson and Logan, 2010).

The concentration of biomass and substrate (lactate) was determined by direct measurement of optical density (OD) of the samples, taken from the anode chamber, at a wavelength of 600 nm and 570 nm, respectively, using a spectrophotometer (UV-2100, U.S.A.). The concentration of dissolved oxygen in the cathode chamber was determined by SevenGo® pro Portable Dissolved Oxygen Meter, METTLER TOLEDO®.

The difference between the cathode and anode potentials and the resistance of the external resistor were measured and recorded every one minute using a data acquisition system (LabVIEW™ 10.0). The current through the cell was calculated based on the measured resistance and voltage.

2.1. Model description

The estimation of electrical energy production is one of the primary goals of the modeling of a microbial fuel cell. The electrical current is generated by reduction of substrate in the anode compartment, so it would be beneficial to primarily find a proper consumption rate equation of substrate. This means to start on the complex interactions among different factors in an MFC, it is necessary to describe the biofilm model using mass balance equations.

The model proposed here is applied for the particular case of an MFC fed with lactate working in a batch mode operation by considering the following assumptions:

- It is assumed that the MFC contains three parts: bulk liquid in the anode chamber, biofilm attached to the electrode of anode and bulk liquid in the cathode chamber. A lumped system has been assumed in each part.
- The electrical resistances of electrodes and the ion exchange membrane have been neglected.
- pH is assumed to be constant in the bulk liquid of cathode and anode chambers.
- The whole system is at the constant temperature of 30 °C.

The overall reactions in the system have been assumed as follows:

Half reaction in the anode: The overall chemical reaction that takes place in the MFC is lactate decomposition into H^+ ions, electrons, resulting waste product, and possibly CO_2 and water.

$$C_3H_6O_3 + 3H_2O \rightarrow 3CO_2 + 12H^+ + 12e^- \quad (1)$$

This would require 3 water molecules to be broken down in addition to the lactate itself, and would produce a total of 12 mol of e^- and H^+ ions per mole of lactate.

Half reaction in the cathode: The reduction of dissolved oxygen in the cathode is suggested as:

$$O_2 + 4H^+ + 4e^- \rightarrow 2H_2O \quad (2)$$

The oxygen molecule is reduced to two water molecules via the transfer of four protons and four electrons.

2.2. Kinetic equation of substrate in anode chamber

The concentration of substrate plays an important role in the determination of the rate of biological processes. The kinetic model of substrate is defined as follows:

$$r_s(t) = \frac{dC_S(t)}{dt} = \mu\phi_a(t) \quad (3)$$

where r_s is the substrate consumption rate in the anode chamber, ϕ_a is the volume fraction of the active biomass, μ is the specific growth rate and C_S is the substrate (lactate) concentration. It is important to note that the substrate consumption rate is a function of substrate concentration and the volume fraction of active biomass.

The specific growth rate is evaluated by three kinetic models. The first model is Monod equation empirically fits a wide range of data satisfactorily and is the most commonly applied unstructured, unsegregated model of microbial growth (Shuler and Kargi, 2002).

$$\mu = r_{max}\frac{C_S}{K_s + C_S} \quad (4)$$

where C_S, r_{max} and K_s are the substrate concentration, reaction rate constant and substrate saturation constant, respectively.

The second model is Blackman model, which is presented as (Zacharof and Lovitt, 2013)

$$\mu = r_{max}\frac{C_S}{2K_s} \quad (5)$$

The third model is Tessier model, which is expressed as follows (Jafary et al., 2013):

$$\mu = r_{max}\left(1 - e^{-\frac{C_S}{K_s}}\right) \quad (6)$$

In the MFC, electron donor (substrate) and electron acceptor (conductive biofilm) have considerable effect in substrate consumption and the rate of electron generation. Accordingly, by combining Nernest and Monod equations, the rate of substrate consumption would be achieved as follows (Marcus et al., 2007; Merkey and Chopp, 2012):

$$r_s(t) = \mu\left(\frac{1}{1 + exp\left(-\frac{F}{RT}\eta_{act}\right)}\right)\phi_a \quad (7)$$

where η_{act} is the activation overpotential, F is Faraday constant, R is the universal constant of gases, and T is the temperature.

2.3. Mass balance in the biofilm

It is assumed that the substrate is diffused from the bulk liquid to the biofilm and then oxidized by the active biomass. The produced CO_2 and H^+ are diffused back to the bulk liquid. Therefore the mass balance of five species exist in the biofilm; active biomass, inactive biomass, substrate, CO_2 and H^+, must be presented (Kazemi et al., 2015).

- Mass balance of the active biomass:

$$\begin{cases} \frac{d}{dt}(A_m\rho\phi_a(t)L(t)) = \text{growth rate} - \text{inactivation rate} + \text{detachment rate} \\ \frac{d}{dt}(A_m\rho\phi_a(t)L(t)) = Y_{ac}r_s(t)A_m\rho L(t) - b_{ina}\rho A_m L(t)\phi_a(t) + \delta(t)A_m\rho\phi_a(t) \end{cases} \quad (8)$$

where $L(t)$ is thickness of biofilm, Y_{ac} is the bacterial yield, A_m is the area of biofilm interface, ρ is the biomass density, b_{ina} is the inactivation coefficient and $\delta(t)$ is the detachment rate which can be calculated by (Wanner and Gujer, 1986)

$$\delta(t) = -b_{det}L(t) \quad (9)$$

where b_{det} is the detachment coefficient. Using the chain rule, Eq. (8) could be reduced to:

$$\frac{d}{dt}(\phi_a(t)) = Y_{ac}r_s(t) - b_{ina}\phi_a(t) + \frac{\phi_a(t)}{L(t)}\delta(t) - \frac{\phi_a(t)}{L(t)}\frac{d}{dt}(L(t)) \quad (10)$$

- Mass balance of the inactive biomass:

$$\begin{cases} \frac{d}{dt}(A_m\rho\phi_i(t)L(t)) = \text{inactivation rate} + \text{detachment rate} \\ \frac{d}{dt}(A_m\rho\phi_i(t)L(t)) = b_{ina}\rho A_m L(t)\phi_a(t) + \delta(t)A_m\rho\phi_i(t) \end{cases} \quad (11)$$

where b_{ina} is the inactivation coefficient. The above equation can be simplified to

$$\frac{d}{dt}(\phi_i(t)) = b_{ina}\phi_a(t) + \delta(t)\frac{\phi_i(t)}{L(t)} - \frac{\phi_i(t)}{L(t)}\frac{d}{dt}(L(t)) \quad (12)$$

By using the assumption of $\phi_a(t) + \phi_i(t) = 1$, we could get the rate of change of the bioflim thickness, as follows:

$$\frac{dL(t)}{dt} = Y_{ac}r_s(t)L(t) + \delta(t) \quad (13)$$

- Mass balance of the substrate:

$$\begin{cases} \frac{d}{dt}(A_m C_S(t)L(t)) = \text{diffusion rate} - \text{consumption rate} \\ \frac{d}{dt}(A_m C_S(t)L(t)) = \frac{A_m D_s}{L_l}(C_{Sb}(t) - C_S(t)) - r_s(t)\rho A_m L(t) \end{cases} \quad (14)$$

where D_s is the effective diffusivity of substrate, L_l is the thickness of the laminar diffusion sublayer, $C_S(t)$ is the concentration of substrate in the biofilm and $C_{Sb}(t)$ is the concentration of substrate in the bulk liquid.

Using the chain rule, Eq. (14) can be reduced to:

$$\frac{d}{dt}(C_S(t)) = \frac{D_s}{L_l L(t)}(C_{Sb}(t) - C_S(t)) - \rho r_s(t) - \frac{C_S(t)}{L(t)}\frac{d}{dt}(L(t)) \quad (15)$$

- Mass balance of the dissolved CO_2:

$$\begin{cases} \frac{d}{dt}\left(A_m C_{CO_2}(t) L(t)\right) = \text{diffusion rate} - \text{consumption rate} \\ \frac{d}{dt}\left(A_m C_{CO_2}(t) L(t)\right) = \frac{A_m D_{CO_2}}{L_l}\left(C_{CO_2 b}(t) - C_{CO_2}(t)\right) + 4r_s(t)\rho A_m L(t) \end{cases} \quad (16)$$

where D_{CO_2} is the effective diffusivity of carbon dioxide, $C_{CO_2}(t)$ is the concentration of carbon dioxide in the biofilm and $C_{CO_2 b}(t)$ is the concentration of carbon dioxide in the bulk liquid.

Using the chain rule, Eq. (16) can be reduced to:

$$\frac{d}{dt}\left(C_{CO_2}(t)\right) = \frac{D_{CO_2}}{L_l L(t)}\left(C_{CO_2 b}(t) - C_{CO_2}(t)\right) + 4\rho r_s(t) - \frac{C_{CO_2}(t)}{L(t)}\frac{d}{dt}\left(L(t)\right) \quad (17)$$

- Mass balance of the hydrogen ion:

$$\begin{cases} \frac{d}{dt}\left(A_m C_H(t) L(t)\right) = \text{diffusion rate} - \text{consumption rate} \\ \frac{d}{dt}\left(A_m C_H(t) L(t)\right) = \frac{A_m D_H}{L_l}\left(C_{Hb}(t) - C_H(t)\right) + 12r_s(t)\rho A_m L(t) \end{cases} \quad (18)$$

where D_H is the effective diffusivity of H^+, $C_H(t)$ is the concentration of H^+ in the biofilm and $C_{Hb}(t)$ is the concentration of H^+ in the bulk liquid.

Using the chain rule, Eq. (18) can be reduced to:

$$\frac{d}{dt}\left(C_H(t)\right) = \frac{D_H}{L_l L(t)}\left(C_{Hb}(t) - C_H(t)\right) + 12\rho r_s(t) - \frac{C_H(t)}{L(t)}\frac{d}{dt}\left(L(t)\right) \quad (19)$$

2.4. Mass balance in the bulk liquid (anolyte)

The volume changes of the bulk liquid ($V_L(t)$) are defined in term of the rate of thickness change of the biofilm as follows:

$$\frac{dV_L(t)}{dt} = -A_m\frac{dL(t)}{dt} \quad (20)$$

It is assumed that the pH of anolyte is constant, therefore the mass of two species; substrate and CO_2, are changing in the anoylate.

- Mass balance of the substrate:

$$\begin{cases} \frac{d}{dt}\left(C_{Sb}(t) V_L(t)\right) = -\text{rate of the biofilm growth} - \text{diffusion rate} \\ \frac{d}{dt}\left(C_{Sb}(t) V_L(t)\right) = -A_m C_{Sb}(t)\frac{dL(t)}{dt} - \frac{A_m D_S}{L_l}\left(C_{Sb}(t) - C_S(t)\right) \end{cases} \quad (21)$$

Using the chain rule, Eq. (21) can be reduced to

$$\frac{d}{dt}\left(C_{Sb}(t)\right) = \frac{1}{V_L(t)}\left(-\frac{A_m D_S}{L_l}\left(C_{Sb}(t) - C_S(t)\right)\right) \quad (22)$$

- Mass balance of dissolved CO_2:

$$\begin{cases} \frac{d}{dt}\left(C_{CO_2 b}(t) V_L(t)\right) = -\text{rate of the biofilm growth} - \text{diffusion rate} \\ \frac{d}{dt}\left(C_{CO_2 b}(t) V_L(t)\right) = -A_m C_{CO_2 b}(t)\frac{dL(t)}{dt} - \frac{A_m D_{CO_2}}{L_l}\left(C_{CO_2 b}(t) - C_{CO_2}(t)\right) \end{cases} \quad (23)$$

Using the chain rule, Eq. (23) can be reduced to

$$\frac{d}{dt}\left(C_{CO_2 b}(t)\right) = \frac{1}{V_L(t)}\left(-\frac{A_m D_{CO_2}}{L_l}\left(C_{CO_2 b}(t) - C_{CO_2}(t)\right)\right) \quad (24)$$

2.5. Mass balance of dissolved oxygen in cathode chamber

It is assumed that the pH is constant in the cathode chamber. Therefore, the only species changes in the cathode chamber are the dissolved oxygen. The mass balance of the dissolved oxygen in the cathode chamber is presented as (Santos et al., 2006):

$$\frac{dC_{O_2}}{dt} = k_L a\left(C_{O_2}{}^* - C_{O_2}\right) - q_{O_2} C_{O_2} \quad (25)$$

where C_{O_2} is the dissolved oxygen concentration, $C_{O_2}{}^*$ is the equilibrium or saturation concentration of the dissolved oxygen, $k_L a$ is the overall volumetric oxygen mass transfer coefficient and q_{O_2} is the specific uptake rate of oxygen. The first and second terms on the right hand side of Eq. (25) represent the oxygen transfer rate (OTR) and the oxygen uptake rate (OUR), respectively.

2.6. Electrochemical model

Real voltage of MFC is less than theoretical one. This decrease is caused by ohmic, concentration, and activation overpotentials as follows (Logan, 2008):

$$E_{output} = E_{thermo} - \eta_{ohm} - \eta_{con} - \eta_{act} \quad (26)$$

The theoretical voltage is the potential difference between the anode and cathode. Where the voltage of anode and cathode are defined as follows (Logan, 2008):

$$E_{cathode} = E_{0,cathode} - \frac{RT}{mF}\ln\left(\frac{1}{C_{O_2} C_{Hc}^4}\right) \quad (27)$$

$$E_{anode} = E_{0,anode} - \frac{RT}{nF}\ln\left(\frac{C_{CO_2}^3 C_H^{11}}{C_S}\right) \quad (28)$$

where m and n are the number of electrons transferred in the reaction of cathode and anode electrodes, respectively. C_{HC} is the concentration of hydrogen ion in the cathode chamber, which assumed constant, $E_{0,anode}$ and $E_{0,cathode}$ are the standard cell electromotive forces of anode and cathode chamber, respectively.

The activation overpotential is defined as (Katuri and Scott, 2011):

$$\eta_{act} = \frac{b}{2.303}\sin\ h^{-1}\left[\frac{i}{2i_{0,ref} C_S}\right] \quad (29)$$

where b is the Tafel coefficient, i is the current and $i_{0,ref}$ is the exchange current in reference conditions.

The ohmic overpontential can be calculated by Ohm law through Eq. (30) (Zeng et al., 2010):

$$\eta_{ohm} = \left(\frac{d_m}{k_m} + \frac{d_{cell}}{k_{aq}}\right) i \tag{30}$$

where d_m is the membrane thickness, d_{cell} is the distance between electrodes, k_m is the membrane conductivity, and k_{aq} is the solution conductivity (Zeng et al., 2010).

The concentration overpotential can be determined through Eq. (31) (Basu and Basu, 2013):

$$\eta_{con} = \frac{RT}{nF} ln\left(\frac{i_l}{i_l - i}\right) \tag{31}$$

where i_l is the limited current of mass transfer which can be calculated through Eq. (32) (Basu and Basu, 2013):

$$i_l = \frac{nFD_s C_{Sb}}{L_l} \tag{32}$$

2.7. Parameter estimation method

Some parameters of the proposed model are estimated based on the experimental data. The method of nonlinear least square is used for estimation of these parameters. The objective function is defined as:

$$J = \sum_{i=1}^{k} (X_{calculted(i)} - X_{experimental(i)})^2 \tag{33}$$

The accuracy of the estimation is calculated by mean square error (*MSE*), root mean square error (*RMSE*) and the coefficient of determination (R^2). *MSE*, *RMSE* and R^2 are calculated as follow:

$$MSE = \frac{\sum_{i=1}^{k} \left(X_{experimental(i)} - X_{calculted(i)}\right)^2}{k} \tag{34}$$

$$RMSE = \sqrt{\frac{\sum_{i=1}^{k} \left(X_{experimental(i)} - X_{calculted(i)}\right)^2}{k}} \tag{35}$$

$$R^2 = \frac{\sum_{i=1}^{k} (X_{experimental(i)} - \bar{X}_{experimental(i)})(X_{calculted(i)} - \bar{X}_{calculted(i)})}{\left(\sum_{i=1}^{k} (X_{experimental(i)} - \bar{X}_{experimental(i)})^2\right)^{0.5} \left(\sum_{i=1}^{k} (X_{calculted(i)} - \bar{X}_{calculted(i)})^2\right)^{0.5}} \tag{36}$$

where $X_{experimental(i)}$ is the measured value; $\bar{X}_{experimental(i)}$ is the mean of measured value; $X_{calculted(i)}$ is the predicted value; $\bar{X}_{calculted(i)}$ is the mean of predicted value and k is the number of observations.

3. Results and discussion

As mentioned before, the proposed model has many parameters. Some of the required parameters are estimated based on the experimental data and the others are selected from the literatures. The value of the model parameters is shown in Table 1.

In the reminder of this section, the results and accuracy of the estimated parameters are presented first, and then, the current and voltage predicted by the model are compared with the experimental data.

3.1. The estimation of kinetic parameters in the anode chamber

Three kinetic models of Monod, Blackman and Tessier are used for calculation of specific growth rate. These models have two parameters, r_{max} and K_s. The experimental data needed for estimation and validation of these parameters are prepared from two experiments. The first experiment, which is used for estimation, was done at lactate concentration of 5.0 kg m^{-3} and the second experiment, which is used for validation, was done at lactate concentration of 7.5 kg m^{-3}. The predicted values of lactate concentration in anolyte solution, using three selected kinetic models and experimental data in both estimation and validation cases, are shown in Fig. 2a–c. In addition, the estimated kinetic parameters, and statistic characteristics are presented in Table 2.

As can be seen from the results, the Monod model is found to fit the experimental lactate concentration well with high coefficients of determination (R^2) of 0.9924 and 0.9861 for estimation and validation, respectively. Although Blakman and Tessier models are found to have a good performance in parameter estimation, but do not have acceptable performance in parameter validation. Thus the Monod model is recommended for the calculation of specific growth rate in MFC.

3.2. The estimation of parameters of oxygen consumption rate in cathode chamber

The oxygen consumption rate in the cathode chamber (Eq. (25)) has two parameters, k_La and q_{O_2}. The experimental data needed for estimation these parameters are prepared from the following experiment. The air was injected into the cathode chamber by an air-pump with the flow rate of 8×10^{-4} m^3 min^{-1}. After reaching to the steady state condition of the dissolved oxygen (7.26×10^{-3} kg m^{-3}), air supplying was stopped. The oxygen concentration began to decrease and after 5 h reached to the concentration of 3.63×10^{-3} kg m^{-3}. Then, by resupplying the air, oxygen concentration increased and approached to a constant value. The predicted values of dissolved oxygen concentration and experimental data are shown in Fig. 3. In addition, the estimated parameters, k_La and q_{O_2}, and statistic characteristics are presented in Table 3.

The results show an excellent agreement between the predicted and experimental values of dissolved oxygen concentration in cathode chamber.

3.3. Validation of the proposed model

The proposed model contains ten ordinary differential equations (Eqs. (10), (12), (13), (15), (17), (19), (20), (22), (24) and (25)) and nine algebraic equations (Eqs. (7), (9), (26)–(32)). These set of differential-algebraic equations are solved by Ode23 solver in MATLAB ver2014. The numerical values of the physical coefficients and biochemical parameters of the model are shown in Table 1. To validate the predictions of the proposed model, the voltage and current of the MFC are measured with time.

The measured and predicted values of voltage and current for lactate concentrations of 5 and 7.5 kg m^{-3} as a function of time are shown in Figs. 4 and 5, respectively. As can be seen from the results, excellent agreement between the predicted and experimental values exists.

Table 1 – Numerical values of the model parameters.

Symbol	Amount	Unit	Ref.
D_s	0.2544×10^{-4}	$m^2\ day^{-1}$	Calculated based on Stewart (2003)
L_l	2×10^{-4}	m	Merkey and Chopp (2012)
ρ	50	$kg\ m^{-3}$	Merkey and Chopp (2012)
Y_{ac}	0.212	kg dry cell kg lactate^{-1}	Tang et al. (2007)
b_{ina}	0.02	day^{-1}	Sedaqatvand et al. (2011)
b_{det}	0.05	day^{-1}	Sedaqatvand et al. (2011)
D_{CO_2}	0.9960×10^{-4}	$m^2\ day^{-1}$	Calculated based on Stewart (2003)
D_H	2.3328×10^{-4}	$m^2\ day^{-1}$	Calculated based on Stewart (2003)
A_m	54×10^{-4}	m^2	Constant
F	96450	$C\ mol^{-1}$	Picioreanu et al. (1999)
T	303	K	Logan et al. (2006)
R	8.314	$J\ mol^{-1}\ K^{-1}$	Constant
V_c	135×10^{-6}	m^3	Constant
V_a	135×10^{-6}	m^3	Constant
$E_{0,anode}$	340	mV	Constant
$E_{0,cathode}$	1299	mV	Logan (2008)
$i_{0,ref}$	0.001	mA	Logan (2008)
b	120	mV	Logan et al. (2006)
d_{cell}	2.5×10^{-2}	m	Haverkamp et al. (1977)
k_{aq}	3500	$mS\ m^{-1}$	Constant
E_{KA}	−155	mV	Measured
d_m	4.5	m	Tang et al. (2007)
k_m	1.7	$mS\ m^{-1}$	Constant
$C_{O_2}{}^*$	7.26×10^{-3}	$kg\ m^{-3}$	Constant
$k_L a$	414	day^{-1}	Estimated
q_{O_2}	2.64	day^{-1}	Estimated
r_{max}	4.20	h^{-1}	Estimated
K_s	1.27×10^{-3}	$kg\ m^{-3}$	Estimated

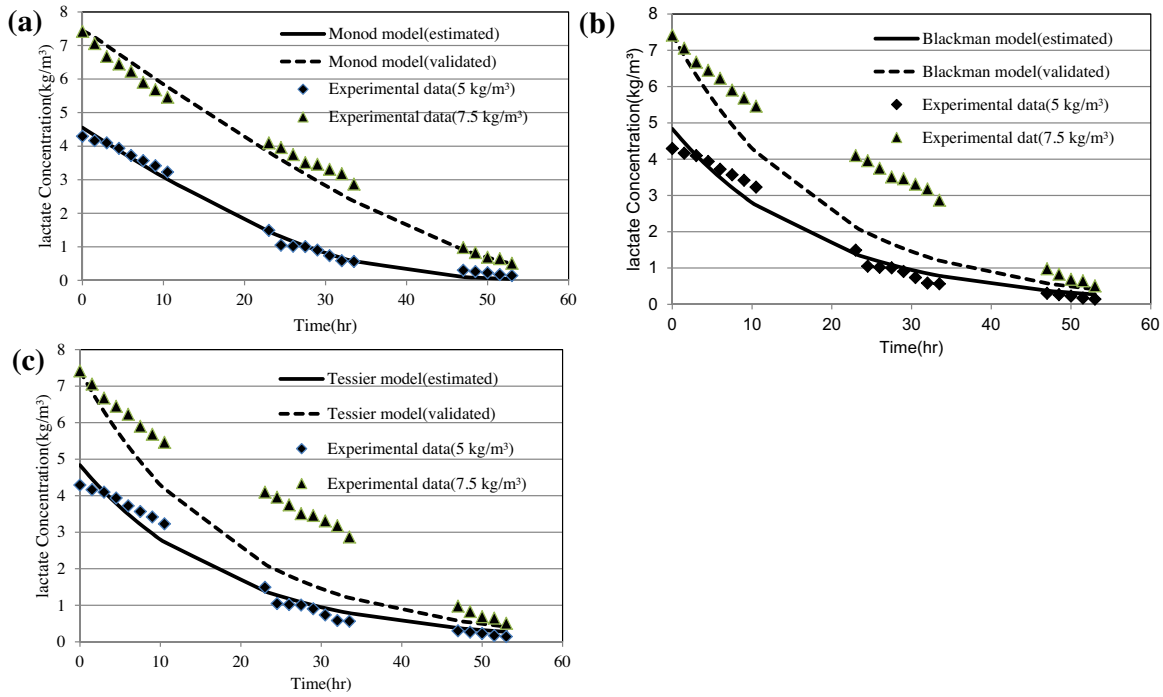

Fig. 2 – Lactate concentration versus time for (a) Monod model (b) Blackman model (c) Tessier model.

Table 2 – The estimated kinetic parameters of anode chamber, and its statistic characteristics.

Model	r_{max} (day^{-1})	K_s ($kg\ m^{-3}$)	Estimation			Validating		
			MSE	RMSE	R^2	MSE	RMSE	R^2
Monod	100.9	1.27×10^{-3}	0.0239	0.1544	0.9924	0.1085	0.3295	0.9861
Blakman	73.92	0.78×10^{-3}	0.0744	0.2728	0.9759	1.6186	1.2723	0.8980
Tessier	97.92	5.16×10^{-3}	0.0670	0.2588	0.9759	1.6262	1.2752	0.8979

Table 3 – The estimated parameters of oxygen consumption rate in cathode chamber.

	k_La (day^{-1})	q_{O_2} (day^{-1})	MSE	RMSE	R^2
Dynamic model	414	2.64	0.1260	0.3175	0.9631

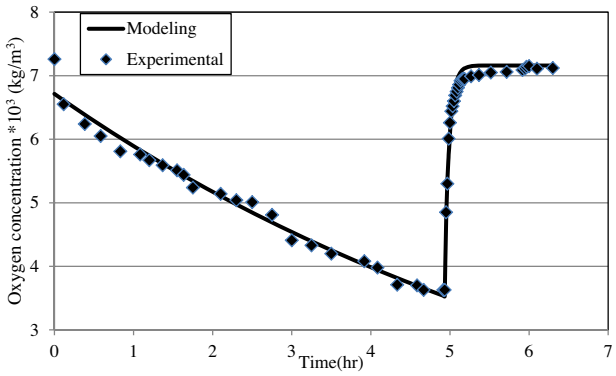

Fig. 3 – Experimental and predicted values of dissolved oxygen concentration in cathode chamber.

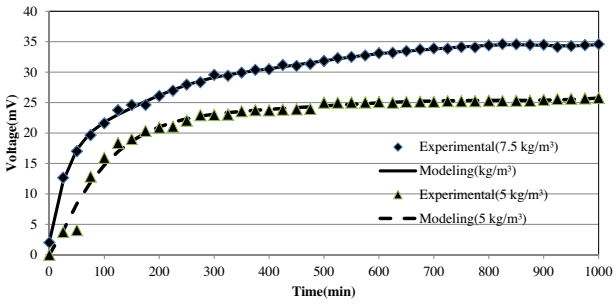

Fig. 4 – Predicted and experimental values of voltage versus time for lactate concentration of 5 & 7.5 kg m^{-3}.

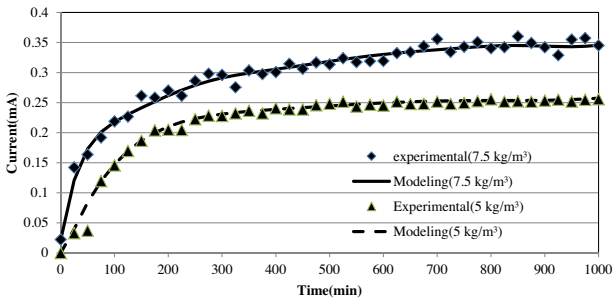

Fig. 5 – Predicted and experimental values of current versus time for lactate concentration of 5 & 7.5 kg m^{-3}.

4. Conclusion

In this paper, a dynamic model has been presented for a batch MFC in constant temperature and the results were compared to the experimental data. In the investigated MFC, lactate was as the substrate, *Shewanella* as the microbial culture, and air as the input feed of the cathode chamber. Some of required parameters of the proposed model were collected from the published literature and the rest were estimated based on the experimental data. The predicted voltage and current of the MFC were compared with the experimental results. There was a good agreement between the experimental data and the results of modeling.

References

Allen, R.M., Bennetto, H.P., 1993. Microbial fuel-cells. Appl. Biochem. Biotechnol. 39, 27–40.

Basu, D., Basu, S., 2013. Mathematical modeling of overpotentials of direct glucose alkaline fuel cell and experimental validation. J. Solid State Electrochem. 17, 2927–2938.

Chaudhuri, S.K., Lovley, D.R., 2003. Electricity generation by direct oxidation of glucose in mediatorless microbial fuel cells. Nat. Biotechnol. 21, 1229–1232.

Chou, T.Y., Whiteley, C.G., Lee, D.-J., Liao, Q., 2013. Control of dual-chambered microbial fuel cell by anodic potential: implications with sulfate reducing bacteria. Int. J. Hydrogen Energy 38, 15580–15589.

Du, F., Xie, B., Dong, W., Jia, B., Dong, K., Liu, H., 2011. Continuous flowing membraneless microbial fuel cells with separated electrode chambers. Bioresour. Technol. 102, 8914–8920.

Esfandyari, M., Fanaei, M.A., Gheshlaghi, R., Mahdavi, M.A., 2016. Neural network and neuro-fuzzy modeling to investigate the power density and Columbic efficiency of microbial fuel cell. J. Taiwan Inst. Chem. Eng. 58, 84–91.

Fitzgerald, L.A., Petersen, E.R., Leary, D.H., Nadeau, L.J., Soto, C.M., Ray, R.I., Little, B.J., Ringeisen, B.R., Johnson, G.R., Vora, G.J., 2013. Shewanella frigidimarina microbial fuel cells and the influence of divalent cations on current output. Biosens. Bioelectron. 40, 102–109.

Haverkamp, R., Vauclin, M., Touma, J., Wierenga, P., Vachaud, G., 1977. A comparison of numerical simulation models for one-dimensional infiltration. Soil Sci. Soc. Am. J. 41, 285–294.

Jafary, T., Ghoreyshi, A.A., Najafpour, G.D., Fatemi, S., Rahimnejad, M., 2013. Investigation on performance of microbial fuel cells based on carbon sources and kinetic models. Int. J. Energy Res. 37, 1539–1549.

Katuri, K.P., Scott, K., 2011. On the dynamic response of the anode in microbial fuel cells. Enzyme Microb. Technol. 48, 351–358.

Kazemi, M., Biria, D., Rismani-Yazdi, H., 2015. Modelling bio-electrosynthesis in a reverse microbial fuel cell to produce acetate from CO_2 and H_2O. Phys. Chem. Chem. Phys. 17, 12561–12574.

Logan, B.E., 2008. Microbial Fuel Cells. John Wiley & Sons.

Logan, B.E., Hamelers, B., Rozendal, R., Schroder, U., Keller, J., Freguia, S., Aelterman, P., Verstraete, W., Rabaey, K., 2006. Microbial fuel cells: methodology and technology. Environ. Sci. Technol. 40, 5181–5192.

Marcus, A.K., Torres, C.I., Rittmann, B.E., 2007. Conduction-based modeling of the biofilm anode of a microbial fuel cell. Biotechnol. Bioeng. 98, 1171–1182.

Merkey, B.V., Chopp, D.L., 2012. The performance of a microbial fuel cell depends strongly on anode geometry: a multidimensional modeling study. Bull. Math. Biol. 74, 834–857.

Min, B., Kim, J., Oh, S., Regan, J.M., Logan, B.E., 2005. Electricity generation from swine wastewater using microbial fuel cells. Water Res. 39, 4961–4968.

Oh, S., Min, B., Logan, B.E., 2004. Cathode performance as a factor in electricity generation in microbial fuel cells. Environ. Sci. Technol. 38, 4900–4904.

Picioreanu, C., van Loosdrecht, M., Heijnen, J., 1999. Multidimensional Modeling of Biofilm Structure. Delft University of Technology, Faculty of Applied Sciences.

Picioreanu, C., Head, I.M., Katuri, K.P., van Loosdrecht, M.C., Scott, K., 2007. A computational model for biofilm-based microbial fuel cells. Water Res. 41, 2921–2940.

Picioreanu, C., Katuri, K., Head, I., Loosdrecht, M.v., Scott, K., 2008. Mathematical model for microbial fuel cells with anodic

biofilms and anaerobic digestion. Water Sci. Technol. 57, 965–972.
Picioreanu, C., Katuri, K.P., van Loosdrecht, M.C., Head, I.M., Scott, K., 2010a. Modelling microbial fuel cells with suspended cells and added electron transfer mediator. J. Appl. Electrochem. 40, 151–162.
Picioreanu, C., van Loosdrecht, M.C., Curtis, T.P., Scott, K., 2010b. Model based evaluation of the effect of pH and electrode geometry on microbial fuel cell performance. Bioelectrochemistry 78, 8–24.
Pinto, R., Srinivasan, B., Manuel, M.-F., Tartakovsky, B., 2010. A two-population bio-electrochemical model of a microbial fuel cell. Bioresour. Technol. 101, 5256–5265.
Pinto, R., Tartakovsky, B., Srinivasan, B., 2012. Optimizing energy productivity of microbial electrochemical cells. J. Process Control 22, 1079–1086.
Potter, M.C., 1911. Electrical effects accompanying the decomposition of organic compounds. Proc. R. Soc. Lond. Ser. B 84, 260–276.
Rabaey, K., Verstraete, W., 2005. Microbial fuel cells: novel biotechnology for energy generation. Trends Biotechnol. 23, 291–298.
Reimers, C.E., Stecher, H.A., Westall, J.C., Alleau, Y., Howell, K.A., Soule, L., White, H.K., Girguis, P.R., 2007. Substrate degradation kinetics, microbial diversity, and current efficiency of microbial fuel cells supplied with marine plankton. Appl. Environ. Microbiol. 73, 7029–7040.
Santos, V., Galdeano, C., Gomez, E., Alcon, A., Garcia-Ochoa, F., 2006. Oxygen uptake rate measurements both by the dynamic method and during the process growth of *Rhodococcus erythropolis* IGTS8: modelling and difference in results. Biochem. Eng. J. 32, 198–204.
Sedaqatvand, R., Esfahany, M.N., Behzad, T., Mardanpour, M., 2011. Comparison of conduction based and mediator based models for microbial fuel cells. J. Petroleum Sci. Technol. 1, 24–29.
Shuler, M.L., Kargi, F., 2002. Bioprocess Engineering. Prentice Hall, New York.
Stein, N.E., Keesman, K.J., Hamelers, H.V., van Straten, G., 2011. Kinetic models for detection of toxicity in a microbial fuel cell based biosensor. Biosens. Bioelectron. 26, 3115–3120.
Stewart, P.S., 2003. Diffusion in biofilms. J. Bacteriol. 185, 1485–1491.
Tang, Y.J., Meadows, A.L., Keasling, J.D., 2007. A kinetic model describing *Shewanella oneidensis* MR-1 growth, substrate consumption, and product secretion. Biotechnol. Bioeng. 96, 125.
Wanner, O., Gujer, W., 1986. A multispecies biofilm model. Biotechnol. Bioeng. 28, 314–328.
Watson, V.J., Logan, B.E., 2010. Power production in MFCs inoculated with *Shewanella oneidensis* MR-1 or mixed cultures. Biotechnol. Bioeng. 105, 489–498.
Wen, Q., Wu, Y., Cao, D., Zhao, L., Sun, Q., 2009. Electricity generation and modeling of microbial fuel cell from continuous beer brewery wastewater. Bioresour. Technol. 100, 4171–4175.
Xuan, J., Leung, M.K., Leung, D.Y., Ni, M., 2009. A review of biomass-derived fuel processors for fuel cell systems. Renew. Sustainable Energy Rev. 13, 1301–1313.
Zacharof, M.-P., Lovitt, R.W., 2013. Modelling and simulation of cell growth dynamics, substrate consumption, and lactic acid production kinetics of *Lactococcus lactis*. Biotechnol. Bioprocess Eng. 18, 52–64.
Zeng, Y., Choo, Y.F., Kim, B.-H., Wu, P., 2010. Modelling and simulation of two-chamber microbial fuel cell. J. Power Sources 195, 79–89.
Zhang, X.-C., Halme, A., 1995. Modelling of a microbial fuel cell process. Biotechnol. Lett. 17, 809–814.

Further reading

http://ptcc.irost.org/.